Microwave propagation with the gas breakdown*

Wang Hui-Hui(王辉辉)†, Liu Da-Gang(刘大刚), Liu La-Qun(刘腊群), and Meng Lin(蒙 林)

School of Physical Electronics, University of Electronic Science and Technology of China, Chengdu 610054, *China*

(Received 5 May 2014; revised manuscript received 21 May 2014; published online 24 September 2014)

By combining the microwave propagation theory and the gas breakdown theory, the microwave propagation with the gas breakdown is analyzed theoretically. Particle-in-cell/Monte Carlo collision (PIC/MCC) simulations are carried out to verify the theoretical results. Based on this theoretical method, the breakdown phenomenon of the pulse microwave is analyzed. The results show that the product values of the initial electron density and the propagation length are the criterion to distinguish the pulse peak decline breakdown and the pulse width reduction breakdown. Furthermore, the energy transmission is also studied, which shows that the total output energy is approximately independent of the input electric field if the electric field is not extremely large.

Keywords: microwave propagation, gas breakdown, particle-in-cell/Monte Carlo collision simulations

PACS: 51.50.+v, 92.60.Ta **DOI:** 10.1088/1674-1056/23/11/115101

1. Introduction

Microwave breakdown is a major issue for high power propagation.[1,2] There have been many models developed for microwave breakdown[3–11] because of its extensive applications in many fields, including plasma propulsion, biomedical applications, and surface treatments.[12–15] However, these models only focus on the effect of the electric field on the ionization collision frequency, and the effect of the electron avalanche on the microwave is not considered. On the other hand, the effect of time-independent plasmas on microwave propagation has also been studied by some scholars.[16–23] However, in microwave breakdown, the plasmas do not preexist but they grow over time owing to the ionization breakdown. Some scholars adopt the finite-difference time-domain method[24,25] to simulate the self-consistent interaction between the microwave propagation and the breakdown. In this paper, a simpler theoretical model of the self-consistent interaction is developed and then verified by PIC/MCC simulations. Due to the simplicity of this model, some interesting physical phenomena are studied theoretically.

A theoretical model of microwave propagation with gas breakdown is presented in Section 2. In Section 3, the continuous microwave is analyzed with this theoretical model, and this is then verified by PIC/MCC simulations. The pulse microwave is presented in Section 4. Furthermore, the energy transmission of both continuous microwaves and pulses is examined in Section 5. Finally, the conclusion is presented in Section 6.

2. Theoretical model of microwave propagation with gas breakdown

When a microwave propagates with gas breakdown, the electron density and the microwave interact with each other. The effect of the electron density on the microwave is presented in Section 2.1, and the effect of the microwave on the electron density is presented in Section 2.2.

2.1. Microwave propagation in plasmas

If the microwave propagates in a space- and time-independent plasma, then the electric field damping is given by[16]

$$|E| = |E_0|\,\mathrm{e}^{-\alpha z}, \tag{1}$$

where

$$\alpha = -\frac{\omega}{c}\,\mathrm{Im}(\sqrt{\varepsilon_\mathrm{r}}),$$
$$\varepsilon_\mathrm{r} = 1 - \frac{\omega_\mathrm{p}^2}{\omega^2+\upsilon_\mathrm{m}^2} - \mathrm{j}\,\frac{\upsilon_\mathrm{m}\omega_\mathrm{p}^2}{\omega(\omega^2+\upsilon_\mathrm{m}^2)}$$

is the relative dielectric constant,

$$\omega_\mathrm{p} = \sqrt{\frac{n_\mathrm{e}e^2}{\varepsilon_0 m}}$$

is the plasma frequency, n_e is the electron density, m is the electron mass, υ_m is the collision frequency, ω is the microwave angular frequency, and ε_0 is the vacuum dielectric constant.

When the microwave propagates with gas breakdown, the electron density n_e is not a constant anymore, which means that α is dependent on t and z. We adopt differential equations

*Project supported by the National Natural Science Foundation of China (Grant No. 11175040).

†Corresponding author. E-mail: whhnjznl@163.com

© 2014 Chinese Physical Society and IOP Publishing Ltd

to describe the effect of t and z. If the group velocity

$$v_{\rm g} = \frac{{\rm d}\omega}{{\rm d}\beta} = \frac{{\rm d}\omega}{{\rm d}\left[\dfrac{\omega}{c}{\rm Re}(\sqrt{\varepsilon_{\rm r}})\right]}$$

is the propagation speed, then equation (1) is rewritten as

$$E_{\rm rms}(t,z) = E_{\rm rms}(t - {\rm d}t, z - v_{\rm g}\,{\rm d}t)\exp[-\alpha(t,z)v_{\rm g}\,{\rm d}t], \quad (2)$$

where $E_{\rm rms}$ is the root-mean-square electric field. If ${\rm d}t$ tends to be 0, then equation (2) can be rewritten as

$$\frac{\partial E_{\rm rms}(t,z)}{v_{\rm g}\partial t} + \frac{\partial E_{\rm rms}(t,z)}{\partial z} = -\alpha(t,z)E_{\rm rms}(t,z). \quad (3)$$

It is worth noting that the reflected wave is not considered in Eq. (3), which is usually minor compared to field attenuation.

Furthermore, if the propagation velocity $v_{\rm g}$ is assumed to be independent of t and z, and τ is defined as $t - z/v_{\rm g}$, then equation (3) is reduced to a more simplified form

$$\frac{\partial E_{\rm rms}(\tau,z)}{\partial z} = -\alpha(\tau,z)E_{\rm rms}(\tau,z). \quad (4)$$

Moreover, the microwave power $|P|$ is proportional to

$$\frac{1}{2}{\rm Re}\{\boldsymbol{E}\times\boldsymbol{H}^*\} = \frac{1}{2}\sqrt{\frac{\varepsilon_0}{\mu_0}}|E_0|^2\,{\rm e}^{-2\alpha z}{\rm Re}\{(\sqrt{\varepsilon_{\rm r}})^*\},$$

and the electron density at the end of the transmission line is usually small, which means that $\varepsilon_{\rm r}$ is roughly 1. Therefore, the output power is expressed as

$$|P| \propto |E_0|^2\,{\rm e}^{-2\alpha z}. \quad (5)$$

2.2. Microwave breakdown ionization

Equation (3) presents the effect of plasmas on field propagation. On the other hand, the effect of the field on plasmas can be solved by gas breakdown theory (Eq. (6)),[3–6] which shows the explosive growth of plasma density along with ionization collision. In Eq. (6), the attachment collision is ignored, which is much smaller than the ionization collision. The diffusion is also ignored, which is much less than the ionization collision when the electric field is much larger than continuous wave breakdown threshold,[6]

$$\frac{\partial n_{\rm e}(t,z)}{\partial t} = \upsilon_{\rm i}(t,z)n_{\rm e}(t,z), \quad (6)$$

where $\upsilon_{\rm i}$ is the ionization frequency and dominated by the electric field.

For the monatomic gas breakdown, $\upsilon_{\rm i}$ can be solved by a Raizer model,[3] which is derived from the continuity equation of the electron energy space. The solution of the Raizer model is shown by Eq. (7)[3,5,6] and the rescaling factor $k_{\rm revise}$ is roughly $k_{\rm r} = 2/\exp[(mu_{\rm d}^2/2E_{\rm ti})^{0.53}/1.7]$ $(mu_{\rm d}^2/2 < 8.6E_{\rm ti})$ obtained by PIC/MCC simulations[6] near the electric field frequency of 2.8 GHz.

$$\begin{cases} \upsilon_{\rm i} = k_{\rm revise}\upsilon_{\rm itheory}, \\ P_{\rm Eav} = \dfrac{e^2E_{\rm rms}^2}{m}\dfrac{\upsilon_{\rm m}}{(\omega^2+\upsilon_{\rm m}^2)}, \\ y = 2\sqrt{\dfrac{3(\upsilon_{\rm itheory}+\upsilon^*)(E_{\rm te}+1)}{2P_{\rm Eav}}}, \\ z = \sqrt{1+\upsilon^*/\upsilon_{\rm itheory}}, \\ \quad {\rm e}^{(a-1)y}\left(\cosh\dfrac{y}{z} + z\sinh\dfrac{y}{z}\right) \\ \quad -{\rm e}^{-(a-1)y}\left(\cosh\dfrac{y}{z} - z\sinh\dfrac{y}{z}\right) \\ = 2a(1+\beta)y + 2\left(1-\dfrac{1}{z^2}\right)\{y\cosh[(a-1)y] \\ \quad +\sinh[(a-1)y] - ay\}, \end{cases} \quad (7)$$

where $E_{\rm ti}$ is the ionization collision threshold energy (15.8 eV for argon[3]), $E_{\rm te}$ is the excitation collision threshold energy, υ^* is the excitation collision frequency, $\upsilon_{\rm itheory}$ is the theoretical ionization collision proposed by Vyskrebentsev and Raizer,[3] $a = \sqrt{(E_{\rm ti}+1)/(E_{\rm te}+1)}$ is roughly 1.2, β is roughly 0.2, and $P_{\rm Eav}$ is the average electric field power. For argon, $E_{\rm te}$ is 11.5 eV, $\upsilon_{\rm m}$ is $7\times10^9 p$, and υ^* is $2.6\times10^8 p$,[3] where p is the pressure in torrs.

The Raizer model shows that $\upsilon_{\rm i}$ is determined by $P_{\rm Eav}$. However, the relation of $\upsilon_{\rm i}$ and $P_{\rm Eav}$ in the Raizer model is apparently too complex to reveal the physical nature. If the excitation collision is not considered, namely, υ^* is zero and β is 1, then the situation is more distinct. Equation (7) is then reduced to $\sinh(ay) = 2ay$, and the ionization collision frequency is reduced to[3]

$$\upsilon_{\rm itheory} = 0.8\frac{P_{\rm Eav}}{E_{\rm ti}+1}.$$

This result means that the ionization frequency is roughly in direct proportion to $P_{\rm Eav}$. Similar results can also be obtained from the energy conversation equation

$$P_{\rm Eav}n_{\rm e} - E_{\rm ti}\upsilon_{\rm i}n_{\rm e} = \frac{\partial(n_{\rm e}\bar{\varepsilon})}{\partial t} = \bar{\varepsilon}\upsilon_{\rm i}n_{\rm e},$$

where $\bar{\varepsilon}$ is the average electron energy, which means

$$\upsilon_{\rm i} = \frac{P_{\rm Eav}}{E_{\rm ti}+\bar{\varepsilon}}.$$

If the excitation collision is considered, then $\upsilon_{\rm i}$ should be less than $0.8P_{\rm Eav}/(E_{\rm ti}+1)$. Some scholars adopt $0.5P_{\rm Eav}/E_{\rm ti}$ to evaluate the ionization frequency approximately for a 10 GHz electric field.[7] However, for a 2.8 GHz electric field, figure 1 shows that $0.3P_{\rm Eav}/E_{\rm ti}$ may be better.

It is worth noting that these models are not always valid for monatomic gases. These models are invalid[6,7] when

$mu_d^2/2$ is much larger than the ionization threshold energy, where u_d is the amplitude of the electron drift velocity.[6] In this situation, σu is about a constant, which means that $\upsilon_i = n_e \sigma u$ is roughly proportional to the pressure p.[7] For argon, υ_i is roughly $2.875 p_{torr}$ GHz.[7] Figure 1 shows this conversion for argon.

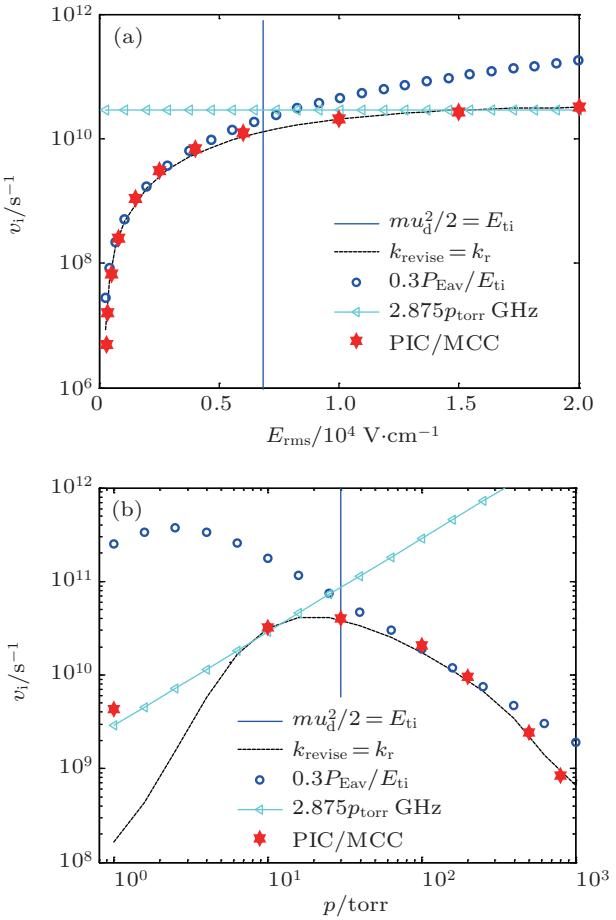


Fig. 1. (color online) Ionization frequency of different models. (a) $f = 2.8$ GHz, $p = 10$ torr; (b) $f = 2.85$ GHz, $E_{rms} = 19.94$ kV/cm. Dark dash line: the result of Raizer model with $k_{revise} = k_r$; the red hexagram: the result of PIC/MCC.[6]

3. Continuous microwave attenuation

Firstly, we calculate the continuous microwave propagation in argon with $\omega = 1.7593 \times 10^{10}$ s^{-1}, $n_e(0,z) = 1 \times 10^9$ m^{-3},[26] $E_{rms}(t,0) = 2 \times 10^3$ V/cm, $p = 10$ torr, and the propagation length $z_d = 60$ mm. In the numerical calculation of the theoretical model, equations (3), (6), and (7) are taken. In addition, simulations are carried out by a PIC/MCC code[6] based on the CHIPIC platform. As in Ref. [6], only elastic momentum transfer collisions, ionization collisions, and excitation collisions are considered. However, the effect of space charge current on the electromagnetic field is also considered[27] in this paper, while this effect is ignored in Ref. [6]. The electric field, power, and electron density of theory at $z = z_d$ are presented in Fig. 2 (the electric field and power are normalized by the input values), which shows that the electromagnetic field fades along with the increase of electron density, and the electron density tends to be a constant when the electric field tends to be zero. Figures 3 and 4 present the according PIC/MCC results of the output electric field and power, which show that the results of theory and PIC/MCC are consistent.

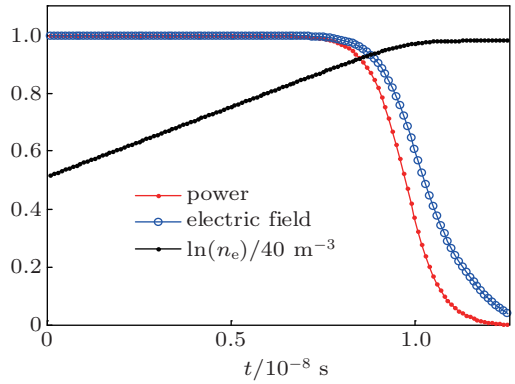


Fig. 2. (color online) Physical quantities of theory at $z = z_d$.

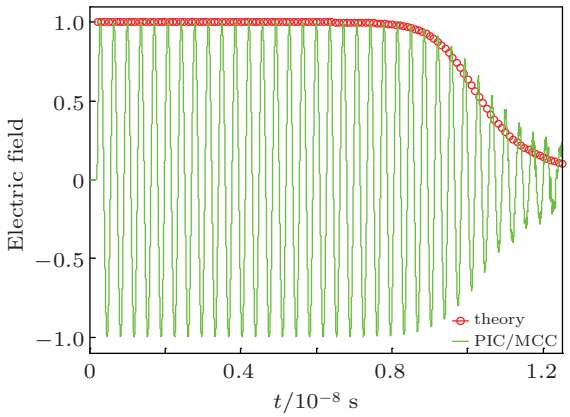


Fig. 3. (color online) Output electric field.

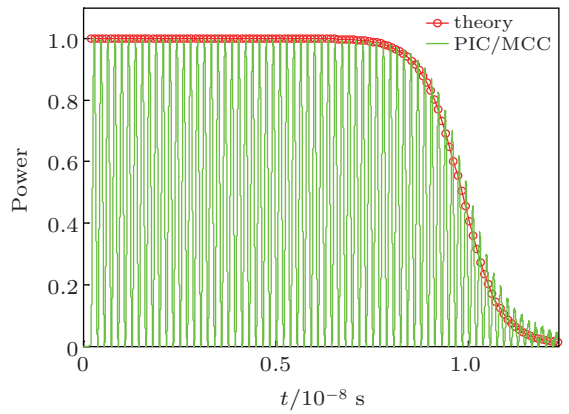


Fig. 4. (color online) Output power.

Physical quantities, not only at $z = z_d$ but also at other places, are also examined. The evolutions of the electric field and electron density distributions are shown in Figs. 5 and 6, respectively. When the field damping does not happen, both

the electric field and the electron density are spatially uniform. However, when the breakdown happens, the electric field damps along the propagation direction, which makes the ionization frequency non-uniform. With the uneven multiplication speed, the electron density at $z = 0$ is much larger than that at other places.

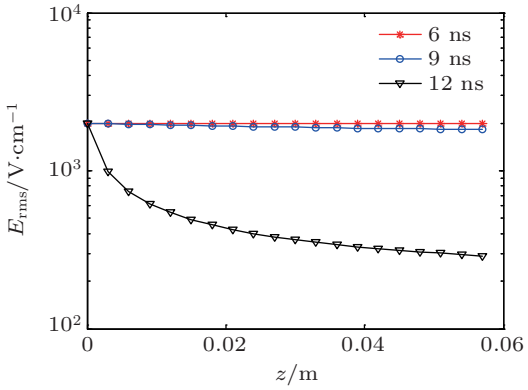


Fig. 5. (color online) Evolution of the electric field distribution.

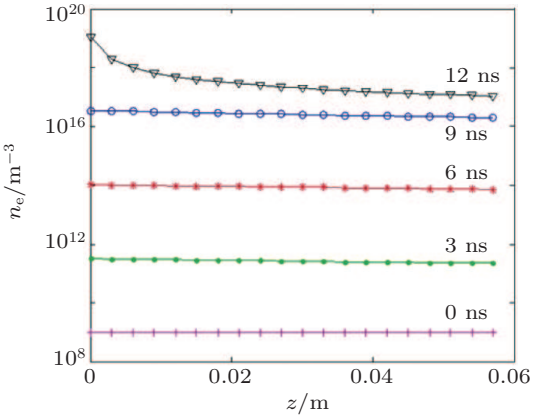


Fig. 6. (color online) Evolution of the electron density distribution.

4. Pulse microwave attenuation

If the pulse width is much larger than the electromagnetic period, then the model in Section 2 is also valid for the pulse microwave propagation. It is clear that both the pulse peak and width decrease when the electric field is extremely large. However, if the electric field is not extremely large, the pulse peak or width may not change, even when the breakdown happens. Phenomenon I is defined as the width decrease with the invariable peak, while phenomenon II is defined as the peak decrease with the invariable width. The criterion to distinguish these two different phenomena is then derived, approximately, below.

We assume that the pulse is symmetric about the peak, which means that the rising time is equal to the falling time. In this situation, the breakdown end time $\tau_{\rm end}$ should be smaller than two times of the breakdown beginning time $\tau_{\rm begin}$ in order to induce phenomenon I, while $\tau_{\rm end}$ should be larger than $2\tau_{\rm begin}$ in order to induce phenomenon II, where $\tau_{\rm begin}$ and $\tau_{\rm end}$ are defined by Eq. (8) according to Eq. (4). Figure 7 shows the sketch map of these two phenomena.

$$\begin{cases} \exp\left(-\int_0^{z_{\rm d}} \alpha(\tau_{\rm begin}, z)\,{\rm d}z\right) = 0.99, \\ \exp\left(-\int_0^{z_{\rm d}} \alpha(\tau_{\rm end}, z)\,{\rm d}z\right) = 0.01. \end{cases} \tag{8}$$

The boundary between these two phenomena can be expressed by

$$\tau_{\rm end} = 2\tau_{\rm begin}. \tag{9}$$

To simplify the derivation process, we assume that $\omega_{\rm p}$ is small, and $\upsilon_{\rm i}(\tau, z)$ is independent of τ and z, and is replaced by a constant $\nu_{\rm i0}$. Then,

$$\begin{aligned} \alpha(\tau, z) &= -\frac{\omega}{c}\,{\rm Im}(\sqrt{\varepsilon_{\rm r}}) \approx \frac{\upsilon_{\rm m}\omega_{\rm p}^2}{2c(\omega^2+\upsilon_{\rm m}^2)} \\ &= \frac{\upsilon_{\rm m}}{2c(\omega^2+\upsilon_{\rm m}^2)}\frac{e^2}{\varepsilon_0 m_{\rm e}} n_{\rm e}(\tau, z) \\ &= \frac{\upsilon_{\rm m}}{2c(\omega^2+\upsilon_{\rm m}^2)}\frac{e^2}{\varepsilon_0 m_{\rm e}} n_0 \exp\left(\int_0^{\tau} \upsilon_{\rm i}(\tau, z)\,{\rm d}\tau\right) \\ &= \frac{\upsilon_{\rm m}}{2c(\omega^2+\upsilon_{\rm m}^2)}\frac{e^2}{\varepsilon_0 m_{\rm e}} n_0\, {\rm e}^{\upsilon_{\rm i0}\tau}. \end{aligned} \tag{10}$$

By combining Eqs. (8)–(10), the boundary value can be obtained as

$$n_0 z_{\rm d} = -\frac{(\ln 0.99)^2/\ln 0.01}{\upsilon_{\rm m} e^2/2c\varepsilon_0 m_{\rm e}(\omega^2+\upsilon_{\rm m}^2)}. \tag{11}$$

Therefore, the necessary condition of phenomenon I is that $n_0 z_{\rm d}$ is less than the boundary value expressed by Eq. (11), while the necessary condition of phenomenon II is that $n_0 z_{\rm d}$ is larger than this boundary value.

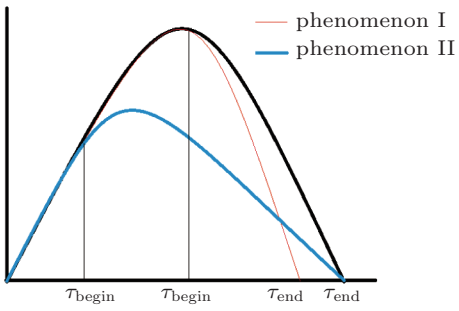


Fig. 7. (color online) Sketch map of phenomenon I and II.

For 10-torr argon, if $\omega = 1.7593 \times 10^{10}$ s^{-1}, and $z_{\rm d} = 0.06$ m, then the boundary value of n_0 is 5.1×10^{12} m^{-3}. If $n_{\rm e}(0, z)$ is set to be 1×10^9 m^{-3}, which is less than the boundary value, and $E_{\rm rms}(t, 0)$ is set to be $3 \times 10^3 \sin(\pi t/t_{\rm dur})$ V/cm, where $t_{\rm dur}$ is 15 ns and t is between 0 and $t_{\rm dur}$, then the output powers of theory and PIC/MCC are presented in Fig. 8(a),

which shows that the breakdown is phenomenon I, as expected (the powers are normalized by the maximum input power). If $n_0 = 1 \times 10^{15}$ m^{-3}, which is larger than the boundary value, and $E_{\rm rms}(t,0) = 1.5 \times 10^3 \sin(\pi t/t_{\rm dur})$ V/cm, then the results are presented in Fig. 8(b), which shows phenomenon II.

If $\omega = 1.7593 \times 10^{10}$ s^{-1}, and $n_{\rm e}(0,z) = 1 \times 10^9$ m^{-3}, then the boundary value of $z_{\rm d}$ is 308 m. If $z_{\rm d}$ is set to be 0.6 m, and $E_{\rm rms}(t,0)$ is set to be $2.55 \times 10^3 \sin(\pi t/t_{\rm dur})$ V/cm, then the results are presented in Fig. 8(c), which shows phenomenon I. If $z_{\rm d}$ is set to be 6×10^5 m, and $E_{\rm rms}(t,0)$ is set to be $1.15 \times 10^3 \sin(\pi t/t_{\rm dur})$ V/cm, then the results are presented in Fig. 8(d), which shows phenomenon II.

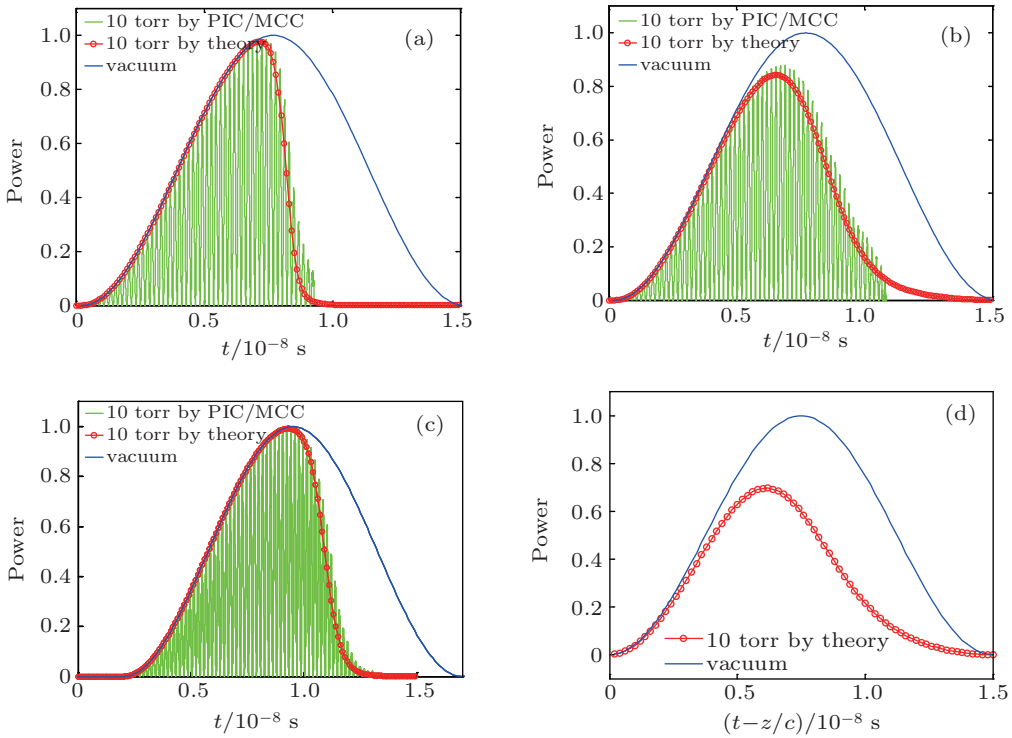


Fig. 8. (color online) Two phenomena of the pulse power attenuation. (a) $n_{\rm e}(0,z) = 1 \times 10^9$ m^{-3} and $z_{\rm d} = 0.06$ m; (b) $n_{\rm e}(0,z) = 1 \times 10^{15}$ m^{-3} and $z_{\rm d} = 0.06$ m; (c) $n_{\rm e}(0,z) = 1 \times 10^9$ m^{-3} and $z_{\rm d} = 0.6$ m; and, (d) $n_{\rm e}(0,z) = 1 \times 10^9$ m^{-3} and $z_{\rm d} = 6 \times 10^5$ m.

5. Energy transmission

Figures 4 and 8 show that the output energy is less than the input energy because of the microwave breakdown. In this section, we discuss the output energy in more detail, the energy is defined as $\int_0^{+\infty} E_{\rm rms}^2 \, {\rm d}\tau$.

5.1. Continuous microwave

Combining Eqs. (8) and (10), the microwave during time $\tau_{\rm end}$ is obtained approximately as

$$\tau_{\rm end} = \upsilon_{\rm i0}^{-1} \ln \frac{\ln 100}{\dfrac{\upsilon_{\rm m}}{2c(\omega^2+\upsilon_{\rm m}^2)} \dfrac{e^2}{\varepsilon_0 m_{\rm e}} n_0 z_{\rm d}}. \tag{12}$$

If $mu_{\rm d}^2/2 < E_{\rm ti}$, then $\upsilon_{\rm i0}$ is roughly

$$0.3 \frac{P_{\rm Eav}}{E_{\rm ti}} = 0.3 \frac{e^2 E_{\rm rms}^2}{m} \frac{\upsilon_{\rm m}}{(\omega^2+\upsilon_{\rm m}^2)E_{\rm ti}},$$

and $\tau_{\rm end}$ is in inverse proportion to $E_{\rm rms}^2$. Therefore, the output energy ($E_{\rm o}$) is roughly independent of the input electric field, which is approximately estimated by Eq. (13), and shown in Fig. 9(a). Although equation (13) is independent of the input electric field, it increases when the pressure increases to the atmosphere pressure, which is shown in Fig. 9(b).

$$\begin{aligned} E_{\rm o} &= \int_0^{+\infty} E_{\rm rms}^2 \, {\rm d}\tau \approx E_{\rm rms}^2 \tau_{\rm end} \\ &= E_{\rm thi} \frac{\ln(2\varepsilon_0 c \ln 100) - \ln\left[\dfrac{e^2}{m_{\rm e}} \dfrac{\upsilon_{\rm m}}{(\omega^2+\upsilon_{\rm m}^2)}\right] - \ln n_0 z_{\rm d}}{0.3 \dfrac{e^2}{m_{\rm e}} \dfrac{\upsilon_{\rm m}}{(\omega^2+\upsilon_{\rm m}^2)}}. \end{aligned} \tag{13}$$

If $mu_{\rm d}^2/2 > E_{\rm ti}$, then $\upsilon_{\rm i0}$ is roughly $2.875 p_{\rm torr}$ GHz (see Fig. 1), and $\tau_{\rm end}$ is independent of the input electric field. Therefore, the output energy is in proportion to $E_{\rm rms}^2$, which is approximately estimated by

$$\begin{aligned} E_{\rm o} &\approx E_{\rm rms}^2 \tau_{\rm end} \\ &= E_{\rm rms}^2 \frac{\ln(2\varepsilon_0 c \ln 100) - \ln\left[\dfrac{e^2}{m_{\rm e}} \dfrac{\upsilon_{\rm m}}{(\omega^2+\upsilon_{\rm m}^2)}\right] - \ln n_0 z_{\rm d}}{18.4 p \times 10^9/6.4}. \end{aligned} \tag{14}$$

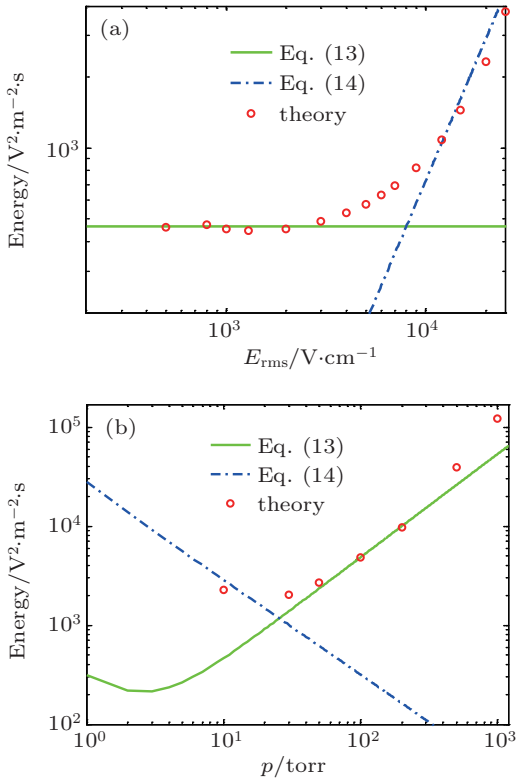


Fig. 9. (color online) Output energy of the continuous microwave for argon with $z_{\rm d} = 0.06$ m, $p = 10$ torr, and $n_{\rm e}(0,z) = 1 \times 10^9$ m^{-3}. The theoretical result is the solution of Eqs. (3), (6), and (7). (a) $f = 2.8$ GHz, $p = 10$ torr; and, (b) $f = 2.85$ GHz, $E_{\rm rms} = 19.94$ kV/cm.

5.2. Pulse microwave

The amplitude of the input electric field in the pulse microwave is varied, which makes the solution more complex. Fortunately, if $mu_{\rm d}^2/2 < E_{\rm ti}$, equation (13) shows that the output energy is roughly independent of the input electric field, which means that the output energy of the pulse should also be the value in Eq. (13). $E_{\rm rms}(t,0)$ is set to be $E_0 \sin(\pi t/t_{\rm dur})$, where t is between 0 and $t_{\rm dur}$, then the results are shown in Fig. 10. When $t_{\rm dur}$ is small, the breakdown does not happen, which means that the output energy is the same as the input energy. Along with the increase of $t_{\rm dur}$, the output energy increases linearly until $t_{\rm dur}$ is large enough to breakdown. When the breakdown happens, the output energy tends to be Eq. (13). If E_0 is small, namely, $mu_{\rm d}^2/2 < E_{\rm ti}$ is always satisfied, equation (13) is its upper limit energy. In contrast, if E_0 is large enough, then $mu_{\rm d}^2/2 < E_{\rm ti}$ is not always satisfied, which means that its upper limit energy increases with the increase of E_0, and is larger than Eq. (13).

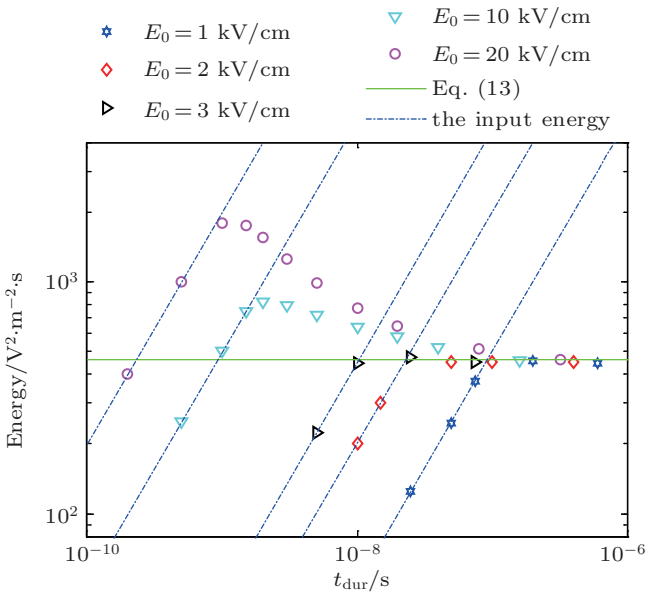


Fig. 10. (color online) Output energy of the pulse microwave for argon with $\omega = 1.7593 \times 10^{10}$ s^{-1}, $z_{\rm d} = 0.06$ m, $p = 10$ torr, and $n_{\rm e}(0,z) = 1 \times 10^9$ m^{-3}. It is worth noting that the results are valid only if $t_{\rm ur}$ is much larger than the electromagnetic period of 0.35714 ns. We present all of our results in Fig. 9 in order to clearly show the rule.

6. Conclusion

In this paper, microwave propagation in gas is described by combining microwave ionization breakdown theory and microwave propagation theory, which is consistent with the result of PIC/MCC. For a continuous microwave, the electron density at z=0 becomes much larger than that at other places after the field attenuation happens (obviously). For the pulse microwave, the decrease of the pulse width with the invariable peak may happen only when $n_0 z_{\rm d}$ is low, while the decrease of the pulse peak with the invariable width may happen only when $n_0 z_{\rm d}$ is high. Furthermore, because of the two different kinds of ionization behaviors, the output energy is almost independent of the input electric field if $mu_{\rm d}^2/2$ is less than $E_{\rm ti}$, while the output energy is almost in proportion to $E_{\rm rms}^2$ if $mu_{\rm d}^2/2$ is larger than $E_{\rm ti}$. Finally, it is worth noting that these results are based on the ionization theory of argon. For other monatomic gases, the results should be similar due to their analogous ionization rules.[3,7] However, for polyatomic gases or mixing gases (such as air), the ionization phenomena are more complex due to their varied excitation collisions. Therefore, we should be cautious when expanding the results of this paper to complex gases.

References

[1] Yang Y M, Yuan C W and Qian B L 2012 *Phys. Plasma* **19** 122101
[2] Krile J T, Neuber A A, Krompholz H G and Gibson T L 2006 *Appl. Phys. Lett.* **89** 201501
[3] Vyskrebentsev A I and Raizer Y P 1973 *J. Appl. Mech. Tech. Phys.* **14** 32
[4] Gould L and Roberts L W 1956 *J. Appl. Phys.* **27** 1162
[5] Wang H, Meng L, Liu D, and Liu L 2014 *Phys. Lett. A* **378** 810
[6] Wang H, Meng L, Liu D and Liu L 2013 *Phys. Plasmas.* **20** 122102
[7] Lau Y Y, Verboncoeur J P and Kim H C 2006 *Appl. Phys. Lett.* **89** 261501
[8] Sorolla E and Mattes M 2010 *IEEE Microw. Rev.* **16** 41
[9] Radmilovic-Radjenovic M and Radjenovic B 2011 *Spectroscopy Letters* **44** 146
[10] Klein T J, Ploch C J, Recknagel C J and Remilard S K 2011 *Appl. Phys. Lett.* **99** 121503
[11] Malik H K and Aria A K 2013 *Appl. Phys. Lett.* **20** 082125
[12] Kwon H C, Won I H and Lee J K 2012 *Appl. Phys. Lett.* **100** 183702
[13] Boeuf J, Chaudhury B and Zhu G Q 2010 *Phys. Rev. Lett.* **104** 015002

[14] Cook A, Shapiro M and Temkin R 2010 *Appl. Phys. Lett.* **97** 011504
[15] Nam S K and Verboncoeur J P 2009 *Phys. Rev. Lett.* **103** 055004
[16] Zheng L, Zhao Q, Luo X G, Ma P, Liu S Z, Huang C, Xing X J, Zhang C Y and Chen X L 2012 *Acta Phys. Sin.* **61** 155203 (in Chinese)
[17] Thoma C, Rose D V, Miller C L, Clark R E and Hughes T P 2009 *J. Appl. Phys.* **106** 043301
[18] Angus J R, Krasheninnikov S I and Smolyakov A I 2010 *Phys. Plasmas* **17** 102115
[19] Hu X, Jiang Z, Zhang S and Liu M 2007 *Computer Physics Communications* **177** 76
[20] Lu X and Laroussi M 2008 *Appl. Phys. Lett.* **92** 051501
[21] Zhang S, Hu X, Jiang Z, Liu M and He Y 2006 *Phys. Plasmas* **13** 013502
[22] Jiang Z, Hu X, Liu M, Zhang S, He Y and Pan Y 2006 *Plasmas Sci. Technol.* **8** 297
[23] Liu M, Hu X, Jiang Z, Zhang S and Pan Y 2006 *Chin. Phys. Lett.* **23** 410
[24] Ford P J, Beeson S R, Kromphoiz H G and Neuber A A 2012 *Phys. Plasmas* **19** 073503
[25] Yuan Z and Shi J 2014 *Acta Phys. Sin.* **63** 095202 (in Chinese)
[26] Kopiczynski T L, Bogdan M, Kalin A W, Schotzau H J and Kneubuhl F K 1992 *Appl. Phys. B* **54** 526
[27] Wang H, Liu D, Meng L, Liu L, Yang C, Peng K and Xia M 2013 *Acta Phys. Sin.* **62** 015207 (in Chinese)